Parametric Study of Reinforced Metakaolin-Based Geopolymer Concrete against Chloride-Induced Corrosion

Oscar D. Huang¹; Changkyu Kim²; Nathaniel J. Lies³; Homero Castaneda, Ph.D.⁴; and Miladin Radovic, Ph.D.⁵

¹Dept. of Materials Science & Engineering, Texas A&M Univ., College Station, TX. E-mail: ohuang2@tamu.edu

²Dept. of Materials Science & Engineering, Texas A&M Univ., College Station, TX. E-mail: b6031a9@tamu.edu

³Dept. of Materials Science & Engineering, Texas A&M Univ., College Station, TX. E-mail: liesmp@tamu.edu

⁴Dept. of Materials Science & Engineering, Texas A&M Univ., College Station, TX. E-mail: hcastaneda@tamu.edu

⁵Dept. of Materials Science & Engineering, Texas A&M Univ., College Station, TX. E-mail: mradovic@tamu.edu

ABSTRACT

Geopolymers (GP) are aluminosilicate network polymers that have gained interest in recent years as an eco-friendly alterative to ordinary Portland cement (OPC) in transportation infrastructure. This novel material can be processed from waste and/or widely available natural materials under ambient conditions. In this study, a set of rebar-reinforced metakaolin-based geopolymer concrete samples were prepared by mixing aggregate with geopolymer binders having different alkali activators (Na⁺ and K⁺), SiO₂/Al₂O₃ ratios, water/solid ratios, and alkali/aluminum ratios. The concrete samples with rebars were then cured for 14 days before they were exposed to simulated marine environment and monitored with electrochemical methods such as open circuit potential (OCP) and electrochemical impedance spectroscopy (EIS). The results show that the composition of GPs strongly affects their corrosion-inhibiting performance.

INTRODUCTION

Reinforced concrete (RC) is a ubiquitous choice of material for transportation infrastructure due to its low-cost, high compressive strength, and ease of use. The most common concretes are fabricated from ordinary Portland cement (OPC), aggregate and reinforced with steel rebar. Since OPC creates a highly alkaline environment (pH > 12), the steel rebar is able to form a passive layer to minimize the corrosion rate and prolong its integrity (Mehta and Monteiro 2017). However, there are various common aggressive agents (e.g., chloride ions, sulfate ions) that can breakdown the passive layer and/or reduce the pH of OPC, which then causes corrosion in the steel rebar (Kim et al. 2020). The formation of the corrosion product would then induce tensile stresses in the concrete and further compromises the integrity of the structure through cracking and delamination (Goldsberry et al. 2018). To counteract this problem, various approaches have been used to prolong the durability of RC. One of these approaches is to modify the rebar with coatings acting as either a dense barrier (e.g., epoxy) (Goldsberry 2019) or a sacrificial barrier (galvanize with Zn) (Lee and Hiam 1989; Popov 2015) to further reduce the rate at which aggressive agents reach the rebar. Another common approach is to add corrosion inhibiting agents such as calcium nitrate into the cement mixture to reduce the diffusion rate of

the aggressive agents (Goldsberry et al. 2018). All of these methods have proven to be effective to a certain degree, however, corrosion is a persisting problem with steel and researchers are always looking for more effective and innovative ways to prolong its service life.

Another issue with OPC is its impact on the environment during the production process. OPC is the most produced man-made material (3.5 billion tones in 2015), and it is estimated that 5-6% of the anthropological CO₂ emission is due to OPC production (Gartner 2004). The production of OPC is an energy-intensive process that requires high manufacturing temperature in cement kilns (up to 1450°C) and also releases a large amount of CO₂ (Mindess et al. 2003). Recently, a new class of inorganic aluminosilicate polymers known as geopolymers (GPs) have received much attention as an eco-friendly and sustainable alternative to Portland Cement in various transportation infrastructure applications (Shayan 2016). GP is a family of amorphous materials that consists of three-dimensional non-crystalline aluminosilicates network stabilized with alkali cations (Provis and Van Deventer 2009). Chemically, GPs are alkali aluminosilicates with the empirical formula, $M_n[-(SiO_2)_z - AlO_2-]_n \cdot wH_2O$ where M is the alkali metal cation, n is the degree of polymerization, z is the Si/Al ratio, and w is the molar water quantity. The main attraction with GP is that it can be processed with waste materials (e.g., fly ash, steel slag) and/or natural resources (e.g., calcined clay), which are inexpensive and abundant, at room temperature while still have mechanical properties (such as compressive strength) similar to that of OPC (Cheng and Chiu 2003; Hardjito et al. 2004; Xu and Van Deventer 2002). More importantly, studies have shown that the use of GP can reduce CO₂ emission up to 44-64% when compared to the use of OPC (McLellan et al. 2011).

Geopolymer concrete (GPC) has been of interest since the early 2000s and they achieved nowadays strength that is on par with OPC concrete (Hardjito et al. 2005; Hardjito et al. 2004; Hardjito et al. 2004). However, as of 2016, most of the studies focuses on optimizing fly ash (FA)-based GPC while curing them under elevated temperature, which is not ideal for their implementation in transportation infrastructure (Shayan 2016). The main shortcoming with studies that utilize FA is that FA does not have a consistent composition and it can vary a lot depending on the location that it is sourced from. This means that it is usually difficult to reproduce results from different studies. In addition, the price of FA has been surging lately with the increase in demand from the concrete industry and the shift of energy production from coal plants. Metakaolin (MK)-based GP has been more extensively studied in the past few years for a more fundamental understanding on GP since it is a pure aluminosilicate source that is highly reactive and more consistent regardless of the source. Some of the examples of previous studies in MK-bases GPs are physical evolution with temperature (Duxson et al. 2007; Mo et al. 2014; White et al. 2010), formation of crystalline phase (Bell et al. 2009; Zhang et al. 2009), structural studies using nuclear magnetic resonance (NMR) spectroscopy (Duxson et al. 2005). However, there are only a few studies on mechanical properties and long-term durability (Davidovits 2005; Marín-López et al. 2009; Olivia and Nikraz 2012; Rowles and O'Connor 2003; Škvára et al. 2012; Subaer and van Riessen 2007; Zhang et al. 2017). One of the main issues with the durability of concrete structure is the corrosion of steel rebar reinforcement, which is an extensive field of interest in the OPC community (Mehta and Monteiro 2017), but only a few studies addressed the rebar corrosion in reinforced GPC. Some researchers claimed GPC to be better than OPC concrete when it comes to inhibiting corrosion (Davidovits 2005; Provis and Van Deventer 2009). However, out of about half a dozen of papers available in the public domain on rebar corrosion in GPC, some of studies showed no or very little benefit of GP on the corrosion inhibiting performance of reinforced concrete (Babaee and Castel 2016; Chindaprasirt

and Chalee 2014; Gunasekara et al. 2019; Miranda et al. 2005; Reddy et al. 2013; Shaikh 2014; Tennakoon et al. 2017). One of the potential reasons for those conflicting results is that different studies used fly ashes with different compositions to prepare GPs. Another issue that makes it difficult to compare results published in different studies is that all the conclusions were drawn without systematic parametric testing, in order words, none of the studies provide any guidance towards producing better GP to inhibit rebar corrosion. This study aims to provide a systematic approach to understand the effect MK-based GP composition on the corrosion-inhibiting properties in reinforced GPCs.

METHODOLOGY

The GPs used in this study were synthesized using either sodium or potassium hydroxide (Noah Technology, TX), amorphous fumed silicon (IV) oxide (Alfa Aesar, MA) with 350-410 m²/g specific surface area, MetaMax® (BASF Catalysts LLC, NJ) metakaolin, and deionized water. MK was chosen as the aluminosilicate source since it is a relatively pure source of aluminosilicate (with SiO₂/Al₂O₃ ratio equal to 2.05) making it a more ideal GP precursor for the purpose of this research than the more commonly used FA which has higher impurities.

The sodium or potassium hydroxide was first dissolved in deionized water to create a highly alkaline solution. The amorphous fumed silicon oxide was then added to adjust the SiO₂/Al₂O₃ ratio of the final product and create the activating solution for the synthesis of GP. The activating solution was then mixed with MK, in a high-shear mixer for 6 minutes at 400 revolutions per minute (RPM) to create a homogenous mixture, referred to as GP paste. For aggregates, 16 mm and 9.5 mm pea gravel from local vendor (All American Stone & Turf, TX), and ASTM C778 standard sand from Humboldt (Humboldt Mfg. Co., IL) were used. The 2 sizes of pea gravel are used as coarse aggregate in 50/50 ratio. To make GPC, the air-dried aggregates were first measured out and dried mix, then GP paste is added in mixed until every component has been distributed properly to create GPC with the ratio of 1:1.5:2 in terms of dried GP: coarse aggregate: sand. The fresh GPC mixture is then poured into a 101.6 mm cube mold in 2 layers with a steel rebar sitting in the middle. The reinforced concrete samples are cured in a closed, sealed environment for the first 7 days, then they are demolded to cure unsealed at ambient conditions for another 7 days.

Table 1. List of GP compositions examined in this study.

K-GP	Na-GP
K 3(2.5)1	Na 331
K 331	Na 3(3.5)1
K 33(1.2)	Na 3(3.5)(1.2)
K 431	Na 431
K 431	Na 43(1.2)

Since GP has four main ingredients, the number of possible compositions is practically endless. Therefore, we narrowed composition of GPs based on previous work (Huang et al. 2020) to several preliminary compositions because of their good compressive strengths, then the compositions. Note that all GPC samples prepared with different GP compositions are labeled as KXYZ or NaXYZ, where the first letters denote potassium (K) or sodium (Na) while XYZ numbers denote SiO₂/Al₂O₃ ratio, water to solid ratio used to prepare GPC, and Na/Al or K/Al ratio, respectively, in GP binder used for GPCs. For example, GPC sample K421 is sample

prepared with K-activator, and SiO₂/Al₂O₃=4, water/solid ratio=2, and K/Al=1. The compositions can be found in Table 1.

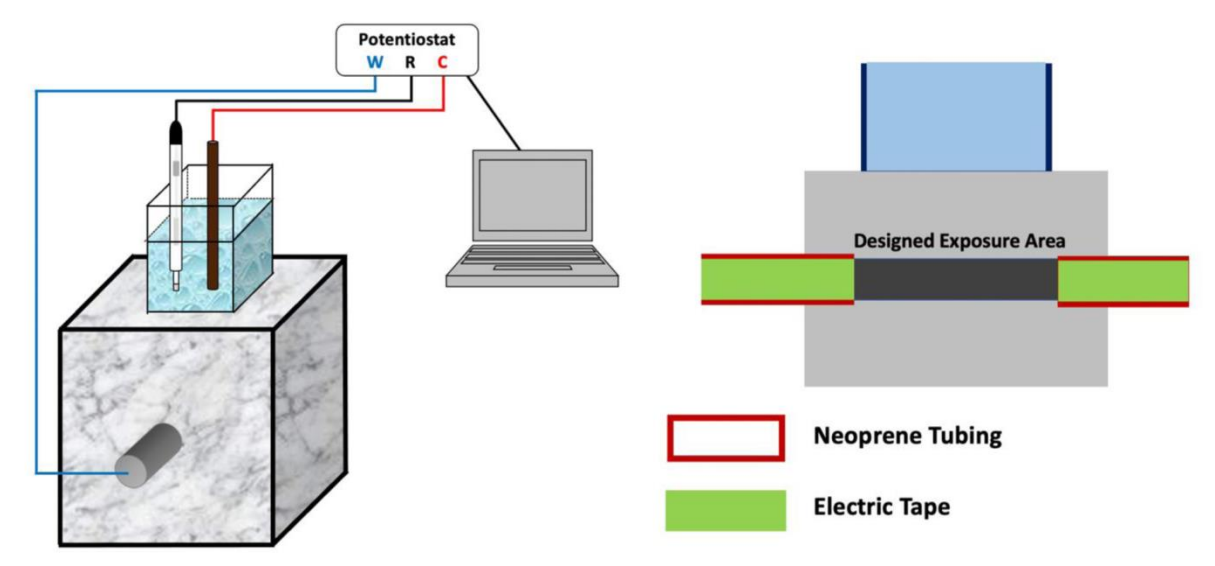


Figure 1. Experimental setup for corrosion testing.

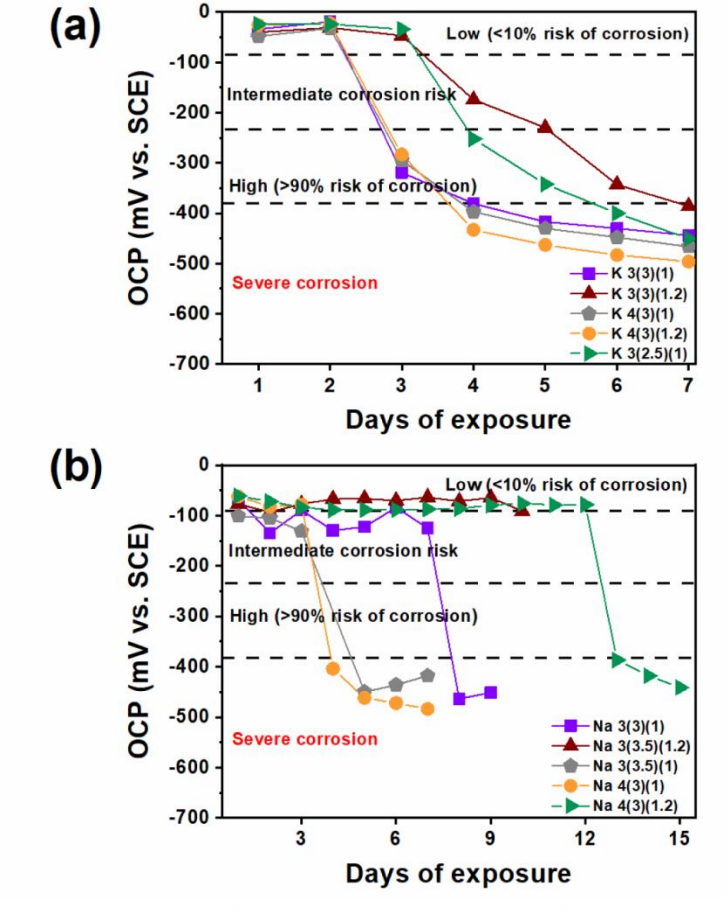


Figure 2. OCP of (a) K-based GPCs and (b) Na-based GPCs during immersion test.

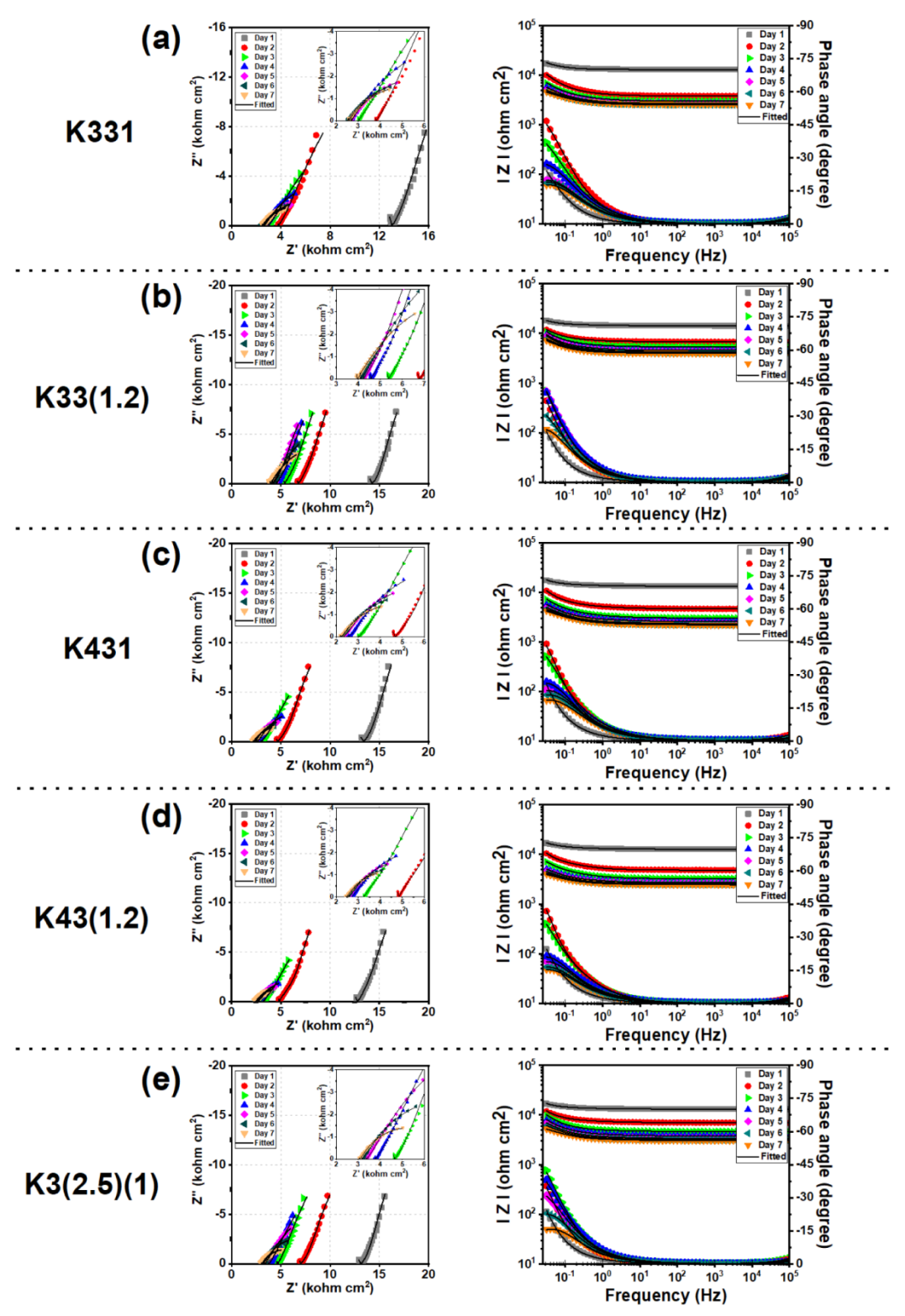


Figure 3. Nyquist (left) and Bode (right) plots of (a) K331, (b) K33(1.2), (c) K431, (d) K43(1.2), and (e) K3(2.5)1.

To properly perform the immersion testing of the GPC specimens, the specimens were prepared by mounting a dam with the electrolyte as shown in Figure 2. The mounting of the dam

was performed after GPC samples were cured for total of 14 days. The specification of the dam area was 50.8 x 50.8 mm² mounted with epoxy resin. The mounted dam was filled with 200 mL 3.5 wt.% NaCl electrolyte to simulate the sea water condition.

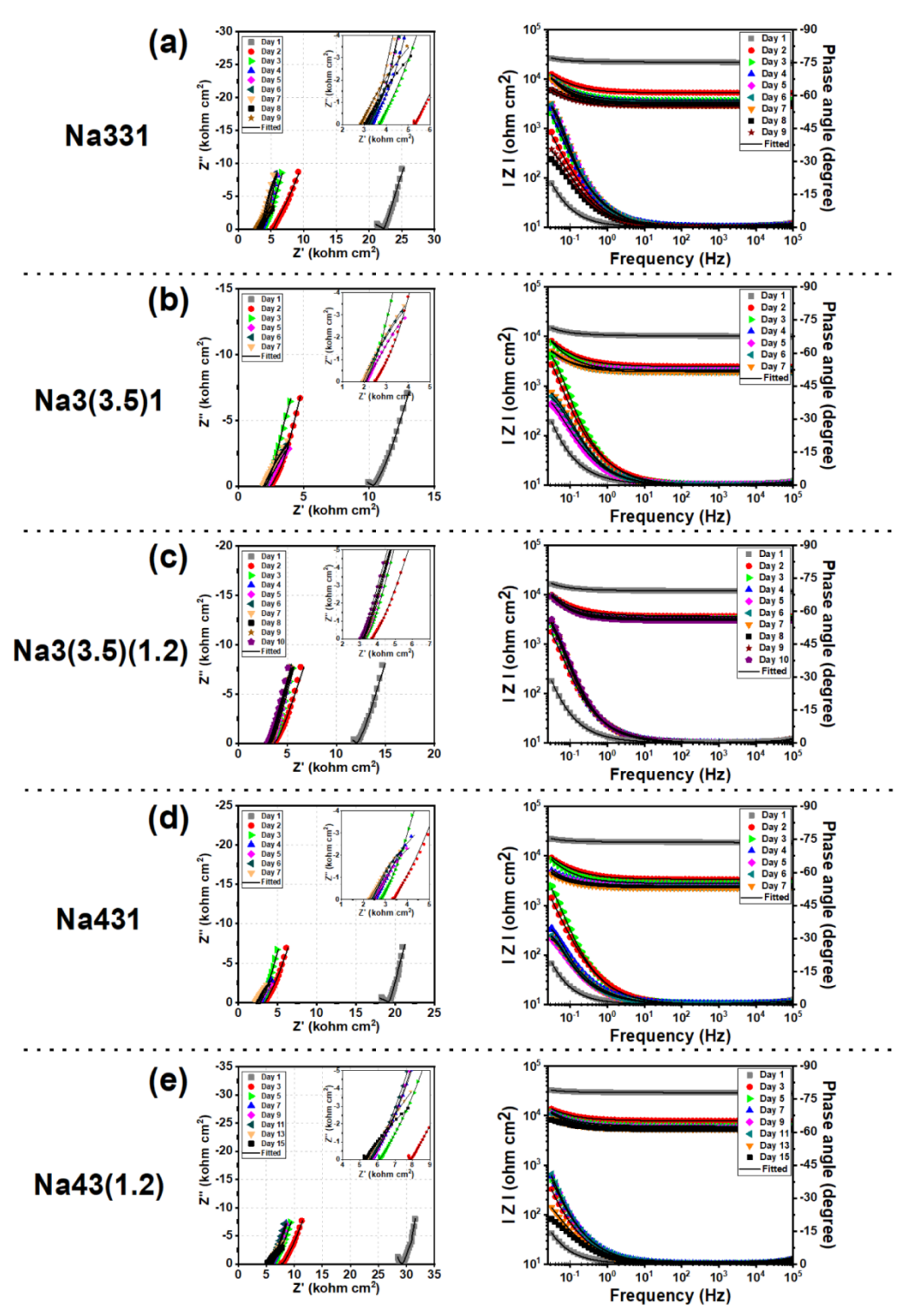


Figure 4. Nyquist (left) and Bode (right) plots of (a) Na331, (b) Na3(3.5)1, (c) Na3(3.5)(1.2), (d) Na431, and (e) Na43(1.2).

The corrosion performance of the produced GPC samples was characterized by EIS as a powerful non-destructive technique that allows the user to monitor, characterize, and determine the performance of the RC system and efficiency in different environments (Castaneda et al. 2018; Cho et al. 2019; Kim et al. 2020). A large number of previously published corrosion results under immersed concrete tests have been analyzed on visual inspection, which is dependent on one's individual viewpoint and could not be explained quantitatively (Aneja et al. 2015; Lee and Hiam 1989; Suay et al. 2003). To overcome the qualitative weakness of visual inspection EIS is utilized to quantitatively monitor the electrochemical processes of the system while it is under constant immersion condition. A three-electrode electrochemical cell was used with the ASTM 615 reinforcing steel (AZZ) as the working electrodes (WE), graphite rod as a counter electrode (CE), and saturated calomel electrode (SCE) as a reference electrode (RE). The test sequence involved 20 minutes of open circuit potential (OCP) measurement followed by EIS with frequency range from 100kHz to 0.03 Hz with 10 logarithmically spaced points per decade with 10 mV rms.

RESULTS AND DISCUSSION

Figure 2 shows the open circuit potential (OCP) trends over the testing period for both K-and Na-based GP concretes. The results from OCP can provide a qualitative indication of the embedded rebar's corrosion activity. The potential difference between the standard reference electrode and the steel rebar as working electrode was used to assess the corrosion of the sample. In this experiment, the criterion suggested previously was applied to understand the regime that the rebar experience (Bertolini et al. 2013).

From Figure 2, it can be observed that the OCP of the K-based samples has a more gradual decrease in OCP values while the Na-based samples which has a more abrupt decrease of the OCP values. This is likely because of the precipitation of the KCl on the surface of the K-based GPC samples which is not observed in the Na-based GPC samples. In another words, the K⁺ in the GP were replaced by the Na⁺ in the electrolyte, which then resulted in the precipitation of KCl. Since Cl⁻ is can destroy the passive layer on the embedded rebar, the precipitation of KCl is beneficial to the protection of the rebar since it decreases the chlorine concentration nearby the rebar so the passive layer can be degraded gradually, however, this means that once the K⁺ has depleted, there would be no more means to protect the rebar. On the other hand, Na-based GPC all exhibit an abrupt decrease of OCP value from low to severe corrosion level within a day. Unlike K-based GPCs, Na-based GPCs have no significant amount of precipitates on the surface after the immersion test. Thus, once the concrete matrix barrier is penetrated by the supplied electrolyte, the rebar reacts with the electrolyte with high chloride concentration that leads to enter the severe corrosion regime directly.

Figure 3 and 4 represent the Nyquist and Bode plots of the tested samples obtained by EIS testing for K-based and Na-based GPCs, respectively. Regardless of the base cation, the early-period Nyquist plots have similar shape as the typical impedance plots for concrete samples. For concrete system, previous study suggests the existence of three elements, namely concrete bulk, bulk-electrode hybrid, and electrode interface (Ford et al. 1998). The charge transfer resistance with double layer capacitance that comes from the reinforcing steel is observable at the low frequency range represented as tail part of the Nyquist plot. It is also noticeable that the real value of the impedance, shown as Z', decreases dramatically after the immersion started, and this is due to the electrolyte uptake through the concrete matrix. Hence, as the electrolyte penetrates more of the concrete matrix, the real part of the impedance decreases and converges to around 3-

5 kohm-cm² at last. Meanwhile, the decrease of corrosion resistance of the rebar is also observable from the decreased impedance modulus and depressed semicircles at the low frequency range of the Nyquist plot. As a result, the water residing inside of the concrete matrix reaches the rebar to initiate the rebar degradation known as corrosion, represented by decreasing size and angle of the tail part of the impedance plot.

The Nyquist plots are in good agreement with the previously shown OCP plots. More specifically, there is no noticeable change with the tail part of the impedance plot before the water reaches the rebar. Thus, the OCP value still maintains at the passive level of low-risk corrosion regime. However, when the water penetrates through the concrete matrix and reaches the rebar, the electrochemical reactions initiate and the breakage of the passivation layer of the rebar occurs, resulting in the gradual decrease of the OCP. This feature is also reflected in the Nyquist plot at the longer period of immersion as the depressed tail part. The depressed part also showed considerably decreased impedance modulus, representative of the decreased corrosion resistance of the system.

As previously mentioned, the different degradation trends of the K- and Na- based GPC samples are also observable in the Nyquist plots. In case of the K-based GPCs, the decrease of the tail part of the impedance plot is gradual as the size of the tail part decreases gradually over time. Meanwhile, in the Na-based GPCs, the decrease of tail part is more abrupt, which is due to of the Cl-concentrated electrolyte uptake to the rebar surface.

Among the K-based GPCs, the K33(1.2) and K3(2.5)1 showed the best anti-corrosion performance. These samples also showed the delayed rebar degradation in the Nyquist and Bode plots compared to the other K-based GPC samples. This result provides some insight for each of the GP parameters in terms of anti-corrosion performance. In terms of SiO₂/Al₂O₃, 3 seems to be better than 4 as observed when comparing between the 2 pairs of compositions – K331 & K431 and K33(1.2) & K43(1.2). In terms of water/solids ratio, K3(2.5)1 shows much better performance when compared with K331, therefore, lower water/solids ratio is better. This is an expected result since lower water/solids ratio in cementitious material has been associated with better mechanical properties, higher density, and lower porosity, however, it should be noted that a minimum water/solids ratio is needed for some minimal fresh workability to prevent the formation mixed-in porosity. In terms of K/Al ratio, 1.2 has showed better performance over 1, indicating the increase in K⁺ improves the GPC's anti-corrosion performance.

In the case of Na-based GPCs, the Na3(3.5)(1.2) and Na43(1.2) showed the best anti-corrosion performance. Those samples also showed the delayed rebar degradation even when compared to the K-based GPCs in all the electrochemical-based tests. Overall, Na-based GPCs show similar trend to K-based GPC in terms of water/solids ratio and Na/Al ratio. However, we do not observe any significant trend with SiO₂/Al₂O₃ for Na-based GPC.

An equivalent circuit (EC) model is suggested as shown in Figure 5 to provide effective parameters for the corrosion of reinforced concrete. The impedance spectra that included the concrete bulk, bulk-electrode hybrid, and electrode interface are allocated for each segment of the equivalent circuit component, respectively. The ECs included elements, namely, the solution resistance (R_s), concrete bulk resistance (R_c), bulk-electrode resistance (R_{be}), charge-transfer resistance (R_{ct}), capacitance in terms of the constant phase element (CPE), concrete bulk pore capacitance (Q_c), bulk-electrode capacitance (Q_{be}), and double-layer capacitance (Q_d). The CPE concept was introduced to represent the depressed impedance semicircles, which is known to be occurred from the various physical properties of the concrete resulting in the time constants distributions (Hirschorn et al. 2010; Hsu and Mansfeld 2001). The CPE capacitance can be

described as below

$$C = Q_0 \left(\omega''_{max} \right)^{n-1}$$
 [1]

where Q_0 and $0 < n \le 1$ are the model parameters, and ω''_{max} is the angular frequency at the maximum imaginary impedance Z''.

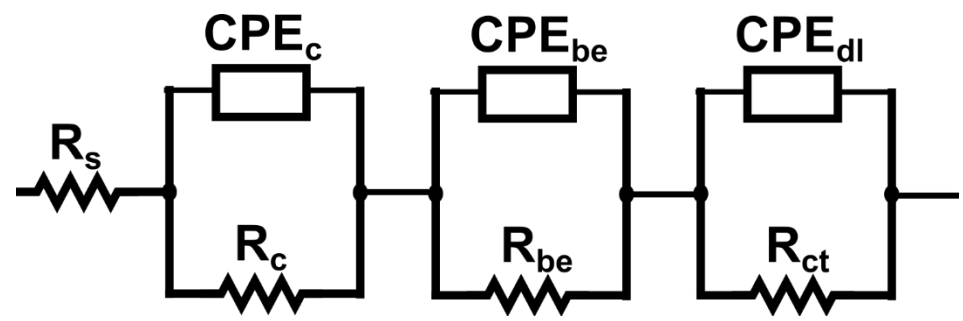


Figure 5. Equivalent circuit for GPC system.

The quantified impedance parameters are obtained from the aforementioned ECs and used to calculate the polarization resistance, R_p. At the initial immersion period, the Na-based GPCs showed a relatively higher R_p, which represents a better barrier performance during this period. The K-based GPC samples have an initial polarization resistance of around 100 kohm-cm², while the Na-based GPC samples generally have higher values up to 140 kohm-cm². Over the prolonged immersion period, the polarization resistance tends to decrease as the water started to penetrate the concrete matrix which is represented as the decrease of concrete bulk resistance and bulk-electrode resistance. The charge-transfer resistance that represents the resistance of the target of interest, such as rebar surface, has been maintained relatively more intact compare to the concrete matrix resistance parameters. Nevertheless, as the water penetrates deeper part of the concrete, the charge-transfer resistance also tended to be decreased over time.

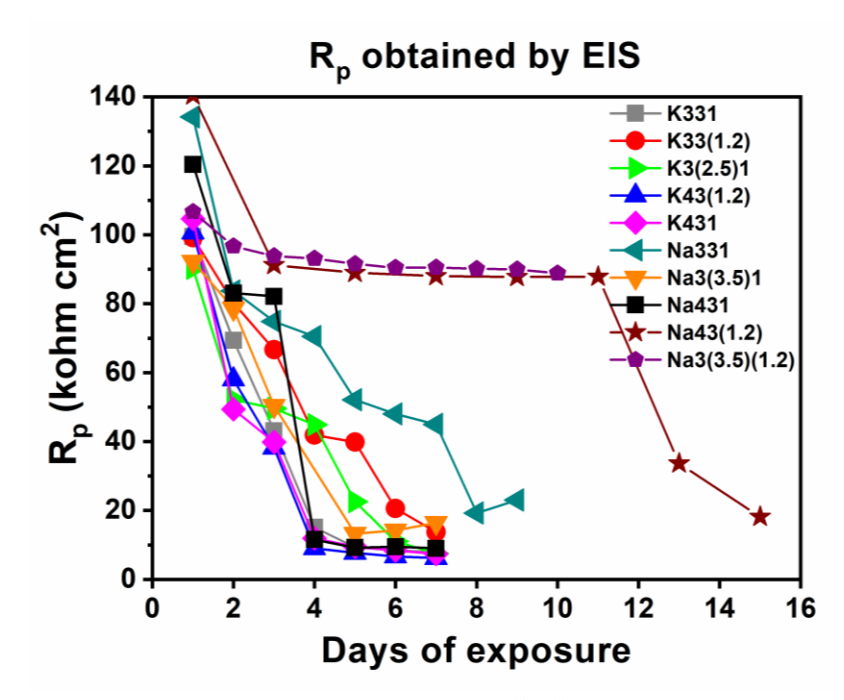


Figure 6. Polarization resistance of the GPCs during immersion test.

As discussed earlier, the decreasing trend of the polarization resistance shows some differences, depending on the type of activation cations in GPC matrix, as it is illustrated in Figure 6. In case of K-based samples, even though its initial polarization resistance was lower than that of the Na-based GPCs, it revealed gradual decrease of the R_p over time similar to the trend that we observed with OCP. Compared to the K-based GPC samples, the Na-based GPC samples showed a relatively better barrier performance since they generally are able to maintain a higher polarization resistance values over a longer period of time. In case of the Na43(1.2), the polarization resistance is maintained at around 92 kohm-cm² range for around 10 days, which is in good agreement with the previous observation that in those samples. This is most likely because the electrolyte starts by gradually penetrating into the outer and easy-to-access pores of the concrete, but then delayed by the inner part of the concrete matrix, so the charge-transfer resistance of the steel rebar itself could be well-maintained until the electrolyte fully penetrates the concrete matrix.

Similar to the trend that we observed with OCP, K-based GPC all demonstrate a gradual decrease in R_p, meanwhile Na-based GPC demonstrate a sudden decrease in R_p into severe corrosion region within a day. Even though K-based GPCs have a more desirable deterioration mechanism, they are not able to protect the rebar for as long as Na-based GPCs are able to. Therefore, a mix-alkali GPC composition could be explored to reconcile the desirable qualities in each of the corresponding compositions.

CONCLUSION AND FUTURE WORK

Durability of reinforced Geopolymer-based Concrete in corrosive environment has been characterized with promising results from the mass transport process mechanism or physical barrier blocking mechanism. The electrochemical results suggest physical barrier mechanism blocking the chloride when the GPC materials are formed, where the mass transport process dominates and the physical results. Overall, Na-based geopolymer shows a much better resistance of chloride-induced rebar corrosion than K-based geopolymer. However, K-based geopolymer seems to allow the rebar to corrode gradually, which is more ideal when compared to Na-based GP, which goes from no corrosion to severe corrosion within a day. Out of all the compositions, Na43(1.2) and Na3(3.5)(1.2) have significantly outperforms the rest of the tested compositions. Therefore, it can be concluded that SiO₂/Al₂O₃ ratio of 3 outperforms 4, and lower water/solids ratio or high alkali/Al ratio produces geopolymer-based cement with better resistance to rebar corrosion. The results of this study can be used as a guidance for future studies to understand how a more optimized GPC composition would compare with OPC under the same condition in the long-term. This would allow us to understand how GPC would perform in real world conditions as marine concrete structure.

REFERENCES

Aneja, K. S., Bohm, S., Khanna, A., and Bohm, H. M. (2015). "Graphene based anticorrosive coatings for Cr (VI) replacement." *Nanoscale*, 7(42), 17879-17888.

Babaee, M., and Castel, A. (2016). "Chloride-induced corrosion of reinforcement in low-calcium fly ash-based geopolymer concrete." *Cement and Concrete Research*, 88, 96-107.

Bell, J. L., Driemeyer, P. E., and Kriven, W. M. (2009). "Formation of ceramics from metakaolin-based geopolymers. Part II: K-based geopolymer." *Journal of the American Ceramic Society*, 92(3), 607-615.

Bertolini, L., Elsener, B., Pedeferri, P., Redaelli, E., and Polder, R. (2013). Corrosion of steel in

- concrete, Wiley Online Library.
- Castaneda, H., Hassan, M., Radovic, M., and Milla, J. (2018). "Self-Healing Microcapsules as Concrete Aggregates for Corrosion Inhibition in Reinforced Concrete."
- Cheng, T.-W., and Chiu, J. (2003). "Fire-resistant geopolymer produced by granulated blast furnace slag." *Minerals Engineering*, 16(3), 205-210.
- Chindaprasirt, P., and Chalee, W. (2014). "Effect of sodium hydroxide concentration on chloride penetration and steel corrosion of fly ash-based geopolymer concrete under marine site." *Construction and Building Materials*, 63, 303-310.
- Cho, S., Chiu, T.-M., and Castaneda, H. (2019). "Electrical and electrochemical behavior of a zinc-rich epoxy coating system with carbon nanotubes as a diode-like material." *Electrochimica Acta*, 316, 189-201.
- Davidovits, J. (2005). Geopolymer, green chemistry and sustainable development solutions: proceedings of the world congress geopolymer 2005, Geopolymer Institute.
- Duxson, P., Lukey, G. C., and van Deventer, J. S. J. (2007). "Physical evolution of Nageopolymer derived from metakaolin up to 1000 °C." *Journal of Materials Science*, 42, 3044-3054.
- Duxson, P., Provis, J. L., Lukey, G. C., Separovic, F., and van Deventer, J. S. (2005). "29Si NMR study of structural ordering in aluminosilicate geopolymer gels." *Langmuir*, 21(7), 3028-3036.
- Ford, S., Shane, J., and Mason, T. O. (1998). "Assignment of features in impedance spectra of the cement-paste/steel system." *Cement and Concrete Research*, 28(12), 1737-1751.
- Gartner, E. (2004). "Industrially interesting approaches to "low-CO2" cements." *Cement and Concrete research*, 34(9), 1489-1498.
- Goldsberry, R., Milla, J., McElwee, M., Hassan, M. M., and Castaneda, H. "Evaluation of Microencapsulated Corrosion Inhibitors in Reinforced Concrete." *Proc., International Congress on Polymers in Concrete*, Springer, 99-105.
- Goldsberry, R. K. (2019). "Electrochemical Evaluation of Self-Healing Epoxy Coated Rebar in Simulated Concrete Pore Solution." Master of Science, Texas A&M University, College Station, TX.
- Gunasekara, C., Law, D., Bhuiyan, S., Setunge, S., and Ward, L. (2019). "Chloride induced corrosion in different fly ash based geopolymer concretes." *Construction and Building Materials*, 200, 502-513.
- Hardjito, D., Wallah, S., Sumajouw, D., and Rangan, B. "Introducing fly ash-based geopolymer concrete: manufacture and engineering properties." *Proc.*, 30th conference on our world in concrete & structures, 23-24.
- Hardjito, D., Wallah, S. E., Sumajouw, D. M., and Rangan, B. V. (2004). "On the development of fly ash-based geopolymer concrete." *Materials Journal*, 101(6), 467-472.
- Hardjito, D., Wallah, S. E., Sumajouw, D. M. J., and Rangan, B. V. (2004). "Factors Influencing the Compressive Strength of Fly Ash-Based Geopolymer Concrete." *Civil Engineering Dimension*, 6, pp. 88-93.
- Hirschorn, B., Orazem, M. E., Tribollet, B., Vivier, V., Frateur, I., and Musiani, M. (2010). "Constant-phase-element behavior caused by resistivity distributions in films: I. Theory." *Journal of The Electrochemical Society*, 157(12), C452.
- Hsu, C., and Mansfeld, F. (2001). "Concerning the conversion of the constant phase element parameter Y0 into a capacitance." *Corrosion*, 57(9), 747-748.
- Huang, O. D., Lies, N. J., and Radovic, M. "Feasibility Study of Metakaolin-Based Geopolymer

- as Binder for Construction Mortar." *Proc., Tran-SET 2020*, American Society of Civil Engineers Reston, VA, 314-323.
- Kim, C., Choe, D.E., Castro-Borges, P., and Castaneda, H. (2020). "Probabilistic Corrosion Initiation Model for Coastal Concrete Structures." *Corrosion and Materials Degradation*, 1(3), 328-344.
- Kim, C., Karayan, A. I., Milla, J., Hassan, M., and Castaneda, H. (2020). "Smart Coating Embedded with pH-Responsive Nanocapsules Containing a Corrosion Inhibiting Agent." *ACS Applied Materials & Interfaces*, 12(5), 6451-6459.
- Lee, H., and Hiam, D. (1989). "Corrosion resistance of galvannealed steel." *Corrosion*, 45(10), 852-856.
- Marín-López, C., Reyes Araiza, J. L., Manzano-Ramírez, A., Rubio Avalos, J. C., Perez-Bueno, J. J., Muñiz-Villareal, M. S., Ventura-Ramos, E., and Vorobiev, Y. (2009). "Synthesis and characterization of a concrete based on metakaolin geopolymer." *Inorganic Materials*, 45(12), 1429-1432.
- McLellan, B. C., Williams, R. P., Lay, J., Van Riessen, A., and Corder, G. D. (2011). "Costs and carbon emissions for geopolymer pastes in comparison to ordinary portland cement." *Journal of cleaner production*, 19(9-10), 1080-1090.
- Mehta, P. K., and Monteiro, P. J. (2017). *Concrete microstructure, properties and materials*, McGraw-Hill Education.
- Mindess, S., Young, J. F., and Darwin, D. (2003). Concrete.
- Miranda, J. M., Fernández-Jiménez, A., González, J. A., and Palomo, A. (2005). "Corrosion resistance in activated fly ash mortars." *Cement and Concrete Research*, 35, 1210-1217.
- Mo, B.-h., Zhu, H., Cui, X.-m., He, Y., and Gong, S.-y. (2014). "Effect of curing temperature on geopolymerization of metakaolin-based geopolymers." *Applied Clay Science*, 99, 144-148.
- Olivia, M., and Nikraz, H. (2012). "Properties of fly ash geopolymer concrete designed by Taguchi method." *Materials & Design* (1980-2015), 36, 191-198.
- Popov, B. N. (2015). Corrosion engineering: principles and solved problems, Elsevier.
- Provis, J. L., and Van Deventer, J. S. J. (2009). *Geopolymers: structures, processing, properties and industrial applications*, Elsevier.
- Reddy, D. V., Edouard, J.-B., and Sobhan, K. (2013). "Durability of Fly Ash—Based Geopolymer Structural Concrete in the Marine Environment." *Journal of Materials in Civil Engineering*, 25, 781-787.
- Rowles, M., and O'Connor, B. (2003). "Chemical optimisation of the compressive strength of aluminosilicate geopolymers synthesised by sodium silicate activation of metakaolinite." *Journal of Materials Chemistry*, 13(5), 1161-1165.
- Shaikh, F. U. A. (2014). "Effects of alkali solutions on corrosion durability of geopolymer concrete." 2, 109-123.
- Shayan, A. (2016). "Specification and use of geopolymer concrete in the manufacture of structural and non-structural components: review of literature."
- Škvára, F., Šmilauer, V., Hlaváček, P., Kopecký, L., and Cílová, Z. (2012). "A weak alkali bond in (N, K)-A-S-H gels: Evidence from leaching and modeling." *Ceramics Silikaty*, 56, 374-382.
- Suay, J., Rodriguez, M., Izquierdo, R., Kudama, A., and Saura, J. (2003). "Rapid assessment of automotive epoxy primers by electrochemical techniques." *Journal of Coatings Technology*, 75(945), 103-111.
- Subaer, and van Riessen, A. (2007). "Thermo-mechanical and microstructural characterisation of

- sodium-poly(sialate-siloxo) (Na-PSS) geopolymers." *Journal of Materials Science*, 42(9), 3117-3123.
- Tennakoon, C., Shayan, A., Sanjayan, J. G., and Xu, A. (2017). "Chloride ingress and steel corrosion in geopolymer concrete based on long term tests." *Materials & Design*, 116, 287-299.
- White, C. E., Provis, J. L., Proffen, T., and Van Deventer, J. S. (2010). "The effects of temperature on the local structure of metakaolin-based geopolymer binder: A neutron pair distribution function investigation." *Journal of the American Ceramic Society*, 93(10), 3486-3492.
- Xu, H., and Van Deventer, J. S. (2002). "Geopolymerisation of multiple minerals." *Minerals Engineering*, 15(12), 1131-1139.
- Zhang, B., MacKenzie, K. J., and Brown, I. W. (2009). "Crystalline phase formation in metakaolinite geopolymers activated with NaOH and sodium silicate." *Journal of materials science*, 44(17), 4668-4676.
- Zhang, M., Zhao, M., Zhang, G., El-Korchi, T., and Tao, M. (2017). "A multiscale investigation of reaction kinetics, phase formation, and mechanical properties of metakaolin geopolymers." *Cement and Concrete Composites*, 78, 21-32.